

Pressure Sounding of the Middle Atmosphere

from ATMOS Solar Occultation Measurements of Atmospheric CO₂ Absorption Lines

M. C. Abrams¹, M. R. G. Sonnerup¹, J. L. Lowes¹, C. P. Rinsland², and R. Zander³

¹Jet Propulsion Laboratory, California Institute of Technology, Pasadena, Ca., 91109, U.S.A.

²Atmospheric Sciences Division, NASA Langley Research Center, Hampton, Va., 23681, U.S.A.

³Institute of Astrophysics, University of Liège, 4000 Liège-Ougrec, Belgium.

Revision Date: 9 September 1994

Proposed Journal: *Applied Optics*

Abstract

A method for retrieving the atmospheric pressure corresponding to the tangent point of an infrared spectrum recorded in the solar occultation mode is described and applied to measurements made by the Atmospheric Trace Molecule Spectroscopy (ATMOS) Fourier transform spectrometer. Tangent pressure values are inferred from measurements of isolated CO₂ lines with temperature-insensitive intensities. Tangent pressures are determined with a spectroscopic precision of 1-3%, corresponding to a tangent point height precision, depending on the scale height, of 70-210 meters. The total uncertainty is limited primarily by the quality of the spectra and ranges between 4-6% (280-420 meters) for spectra with signal to noise ratios of 300:1, to 4-10% for spectra with signal to noise ratios of 100:1. The retrieval of atmospheric pressure increases the accuracy of the retrieved gas concentrations by minimizing the effect of systematic errors introduced by climatological pressure data, ephemeris parameters, and the uncertainties in instrumental pointing.

1. introduction

Remote measurements of the infrared telluric spectrum are a powerful means of studying chemical and dynamical processes in the atmosphere. However, the retrieval of gas concentrations from such spectra depends critically on the knowledge of the observation geometry and the physical characteristics of the atmosphere along the ray path. In limb sounding, precise knowledge of the tangent pressure (or height) for each observation is mandatory for the subsequent determination of accurate gas concentrations (expressed as volume mixing ratio).

The limb sounding geometry may be determined by two different methods: calculation from orbital mechanics and knowledge of spacecraft position and motion, or direct inference from measurements of temperature-insensitive absorption features of gases like CO₂, N₂, and O₂ for which the vertical volume-mixing ratio profile is known¹. In the first method, the motion of the platform versus time as represented by the spacecraft ephemeris yields tangent pressures from climatological models with an accuracy seldom better than ± 1 (E%, which critically limits the accuracy of gas concentration retrievals².

Pressure sounding through the inversion of temperature-insensitive absorption features of atmospheric CO₂ provides an attractive alternative, offering rapid determination of the viewing geometry by application of Beer's law. This method has been used extensively in the analysis of the solar occultation measurements obtained by the ATMOS experiment from three Space Shuttle missions (SPACELAB-3 (1985), ATLAS-1 (1992), and ATLAS-2 (1993)). A general description of the retrieval of the vertical distribution of atmospheric trace constituents from high resolution spectra can be found for example in Brown *et al.*³. The method requires a plausible initial estimate of tangent pressures and temperature profiles which can be obtained from the National Meteorological Center (NMC). While well known, the method has only been described in the interpretation of narrowband radiometric solar occultation measurements⁴. In this paper we describe the method of spectroscopic pressure sounding using high resolution infrared solar occultation absorption spectra obtained by the ATMOS instrument and demonstrate that it can deliver a precision of $\pm 1-3$ % in pressure (70-210 meters in altitude). A total uncertainty of 4-6% can be achieved with spectra of reasonable quality. The self consistency of the method will be assessed and its relative insensitivity to assumptions regarding the atmospheric temperature profile will be examined carefully in terms of the potential for systematic errors in gas concentration profiles.

In certain remote sensing applications it has been necessary to combine the determination of tangent pressure with a simultaneous measurement of the tangent temperature. In the absence of an accurate climatological temperature profile, which was the case for the SPACELAB-3 mission, Rinsland *et al*⁵ derived tangent pressures from a simultaneous measurement of temperature and pressure with an accuracy of 5% using both temperature-sensitive and temperature-insensitive features in the ν_3 band of CO₂. In spectral regions that do not include temperature-insensitive absorption features, pressure sounding using temperature-sensitive absorption features can lead to inaccurate tangent pressure measurements; to address this limitation during the ATLAS-1 mission, Stiller *et al*⁶ derived simultaneous tangent pressures and temperatures from measurements of CO₂ volume mixing ratio profiles using a linear regression technique. Historically, simultaneous measurements of pressure and temperature are computationally very intensive and pressure sounding offers a rapid and accurate alternative that is sufficient for the retrieval of many atmospheric trace gases.

2. The Spectroscopic Retrieval of Tangent Pressure

The method presented has been implemented and evaluated using the observations of the atmosphere made by the ATMOS experiment. ATMOS makes infrared spectroscopic observations of the Earth's atmosphere in a limb-viewing geometry during sunrises and sunsets seen from on board the Space Shuttle from which vertical distribution of more than thirty minor and trace atmospheric constituents have been inferred. An active solar tracker points the ATMOS instrument at the Sun and follows the solar disk during each solar occultation event. The instrument is a Fourier transform spectrometer which measures the mid-infrared spectrum between 625 and 5000 cm⁻¹ (2 - 16 μ m) at 0.01 cm⁻¹ spectral resolution using a series of overlapping broad band interference filters. The high spectral resolution and wide spectral coverage of the instrument allows gas concentration measurements to be made with unblended absorption features that are largely temperature-insensitive. A typical ATMOS occultation consists of approximately 1(K) spectra recorded at time intervals of 2.2 seconds covering the altitude range from the troposphere to the lower thermosphere. For an observation platform in low Earth orbit (altitude \sim 3(K) km) the rate of change of the tangent point altitude is approximately 1 kilometer per second, and consequently tangent height separations of about 2 km are achieved for successive spectra. Each atmospheric spectrum is ratioed to an average of many exo-atmospheric spectra to provide cancellation of the intrinsic instrument and solar features.

Pressure sounding compares an observed spectrum with a calculated spectrum

$$T'_c(\sigma_i, z) = \exp\left(-\sum_{j=1}^m \sum_{k=1}^n \kappa_{ijk} n_k x v_{jk} g_k\right) \quad (1)$$

where σ is the spectral frequency, z is the tangent height, κ_{ijk} is the absorption coefficient for the i th spectral point due to the j th gas in the k th layer, n_k is the number density of air in the k th layer, v_{jk} is the volume mixing ratio of the j th gas in the k th layer, x is a multiplicative scale factor for the volume mixing ratio, and g_k is the geometrical slant path through the k th layer. Each layer is assumed to be homogeneous in temperature, pressure, density, and gas distribution; below 80 km local thermodynamic equilibrium and no wind shears are assumed. The least-squares criterion is used to minimize the sum of the squares of the residual differences between the measured spectrum $T'_m(\sigma_i, z)$ and the calculated spectrum $T'_c(\sigma_i, z)$ convolved with the instrument function, where the residual at the frequency σ_i is

$$r_i = T'_m(\sigma_i, z) - T'_c(\sigma_i, z)^* \quad (2)$$

and the asterisk denotes a convolution. The expression

$$\sum_i \frac{\partial T'_c(\sigma_i, z)}{\partial x} r_i = 0 \quad (3)$$

is implicitly solved for x using a zero crossing search with the partial derivative of the transmission with respect to absorber amount acting as a weighting function in the fitting process.

The random error in a spectroscopic tangent pressure measurement is given by the number of molecules that can be attributed to the residual spectrum relative to the number of molecules that can be attributed to the spectrum (the volume mixing ratio). The precision, or random error, Δ in the retrieved pressure is

$$\Delta = \left[\frac{p(z)}{v(z)} \right] \left[\sum_i \frac{(\partial T'_c / \partial x)^2}{N^2 + r_i^2} \right]^{-1/2} \quad (4)$$

where $p(z)$ and $v(z)$ are the pressure and volume mixing ratio at the observed tangent height z and N is the spectral noise in the measured transmittances. The inclusion of a noise estimate insures that the error is always nonzero and provides a realistic limit for the fitting process. The broadband spectral coverage allows many unblended CO_2 features to be used for the measurement of tangent pressure, with the results of each retrieval combined into a statistical average to obtain a best estimate of the actual tangent pressure and the associated error. A weighted mean and a weighted standard deviation

(lo) represent a realistic translation of the error in the fitting into a measure of the precision of the retrieved quantity,

3. Results and Discussion

Three initial assumptions are necessary to perform a pressure sounding: (1) a plausible model of the atmospheric pressure versus temperature distribution; (2) good knowledge of the vertical concentration distribution of CO₂; (3) and a set of temperature-insensitive spectral absorption features of CO₂ with well characterized line parameters. Each of these assumption is detailed hereafter.

Pressure-temperature profiles, which are model assimilated daily temperature analyses of TIROS Operational Vertical Sounder (TOVS) satellite and radiosonde data⁸, can be obtained from the National Meteorological Center (NMC)⁹. Finger *et al*¹⁰ have determined that the accuracy of the NMC stratospheric temperature analyses is 2-3 K in the lower stratosphere, decreasing towards 10-15 K near the stratopause. Calibration of the NMC satellite data with radiosonde measurements introduces the potential for larger errors over remote locations, such as the oceans in the southern hemisphere where there are fewer radiosonde measurements than over northern hemisphere, continental areas. To provide an extension of the measurements above the stratopause the MSISE-90 model¹¹ provides temperature, pressure, and density conforming to zonal average tabulations¹². The MSISE-90 representation is a purely analytic filling of the tabulated zonal average temperature with a standard deviation of 3K and pressure with a standard deviation of 2% over the 0 to 80 km altitude range, although specific comparisons with NMC profiles for a given place and time suggest that, particularly for the stratopause, the MSISE-90 temperatures are typically 10-20 K higher than the measurements.

A mean CO₂ profile has been assumed for the March-April 1992 ATLAS-1 mission with a constant volume mixing ratio of 347 parts per million by volume (ppmv) in the lower stratosphere, increasing to 360 ppmv in the troposphere. These assumptions resulted from the lower stratospheric measurements of Bischof *et al*¹³ and Schmidt and Khedim¹⁴; an annual increase rate of 1.2 ppmv/year is applied for subsequent missions. An altitude independent volume mixing ratio of 0.7808 parts by volume is assumed for N₂ whose electric quadrupole transitions can be used in the 15-40 km altitude range¹⁵. Nitrogen lines can be used as an independent validation of the tangent pressures determined from the CO₂ transitions.

The assessment of atmospheric pressure is accomplished by the least-squares fitting of the measured spectrum with a calculated spectrum within spectral intervals or *microwindows* containing one or

more absorption features of the desired species. The selection and definition of *suitable* microwindows for this application was based on several criteria: ideally, microwindows about 0.2 to 0.4 cm^{-1} wide were selected to obtain isolated spectral features with well defined 1% transmission levels on either side of the line over the altitude range of interest. Occasionally, the use of wide microwindows, with widths between 1.0 and 10.0 cm^{-1} required that the absorption features of interfering gases be well identified and characterized. Altitude limits were assigned to correspond to central absorptions of typically 2-70 % for the target features. A major consideration was the temperature dependence of the CO_2 absorption features, which is mainly dependent on the lower state energy (E'') of the transitions. With an assumed temperature accuracy of better than 5 K, lines with lower state energies between 60 and 400 cm^{-1} may be used for temperature-insensitive pressure determinations to better than 2%. Microwindows for high resolution pressure sounding from CO_2 lines are listed in Table 1 for the altitude range between 15 and 125 km. In the following discussion attention will be focused on tangent pressure retrievals in the spectral region (1550 - 3450 cm^{-1}) corresponding to one of the optical filters in which the root mean square signal-to-noise ratio in the continuum is typically 90-130. At such a level the noise is a significant component of the random error budget.

The method of pressure sounding has been applied to a large set of observations made by the ATMOS instrument obtained during three Space Shuttle missions in 1985, 1992, and 1993. Results are presented for a typical occultation with an average signal-to-noise ratio of 100:1 and a hemispheric average occultation, in which all sunrise occultations in a given filter are averaged together, with a signal-to-noise ratio of 300:1. These examples represent two extreme cases: in the worst case, the noise is the largest component of the error budget, while in the best case the largest component is the accuracy of the spectroscopic parameters. The pressure errors for a single occultation (Figure 1a) are a statistical average and range from 2-6% in tangent pressure, or 140-440 meters in tangent height (assuming a 7 km scale height), with a near linear dependence on tangent pressure. The presence of an apparent pressure dependence in the tangent pressure error reflects the amount of spectral information available at different tangent pressures. The fractional opacity, defined as the normalized weighted sum of the transmittance within the microwindow increases at lower altitudes, and the presence of more compatible microwindows at lower altitudes combine to decrease the random error in the pressure sounding process. The number of microwindows available at higher altitudes is not sufficient to significantly decrease the random error relative to a single measurement.

Self-consistency dictates that if a tangent pressure is determined assuming a CO_2 volume mixing ratio of 347 ppmv, then within that same spectral microwindow, a burden retrieval of CO_2 should return 347 ppmv, if that retrieved tangent pressure is assumed. The absence of any statistical bias of the mean CO_2 profile with respect to the assumed CO_2 (Figure 1b) profile indicates the robustness of the retrieval process: each retrieved result lies within a fraction of a standard deviation of the expected value and at worst there might be a $\sim 0.5\%$ bias which is relatively small compared with an average weighted standard deviation of 4%. There is an anti-correlation between the pressure error and the number of microwindows (as illustrated in Figure 2) which indicates a statistical (square-root dependence) tendency. To obtain tangent pressure errors that are near constant over the altitude range it is necessary to find enough microwindows at each altitude. This has proven to be impractical above 50 km and leads to the limitation on the precision of the results.

The anti-proportionality between the tangent pressure error and pressure is suggestive that within a single occultation the measurement errors are dominated by the limitations of the finite signal-to-noise ratio, which is typically 100 in the spectral region between 2000 and 4000 cm^{-1} . A zonal or hemispheric average of many occultations can improve the signal-to-ratio by as much as a factor of 5, which should decrease the random error significantly. The tangent pressure retrieval illustrated in Figure 3 is retrieved from a zonal average occultation that combines all sunrise spectra in ATMOS Filter 3 into a single occultation. The results are considerably improved over the individual occultation results: at all tangent pressures the random error lies between $\sim 0.5\%$ and 1.5% . The continued improvement in precision towards lower altitudes remains due to the larger fractional opacity and the presence of more microwindows, but the range of errors is more consistent with the variation in opacity than was observed in either a single microwindow or single occultation retrieval.

An independent validation may be obtained with a retrieval of N_2 using the electric quadrupole transitions that occur in relatively uncluttered spectral regions near 2400 cm^{-1} in the 15 to 40 km altitude range. The spectral intervals and altitude ranges, over which the four best N_2 transitions can be used, are given in Table 2. The results in Figure 4, for both an individual occultation and a zonal mean occultation, confirm that the tangent pressure assignments are spectroscopically consistent with the known volume mixing ratio of N_2 , and that there is no statistical bias of the results due to differences between measurements based on either CO_2 or N_2 . This conclusion is consistent with a previous investigation⁵.

4. The Error Budget

The error budget for tangent pressure sounding must include both random errors that lead to the precision discussed above and systematic errors that, in combination with the random errors, determine the accuracy of the measurements. Sources are quantified in Table 3 and include (1) uncertainties in the assumed temperature profile, (2) the accuracy of the vertical distribution of CO₂, (3) the accuracy of the spectroscopic parameters, (4) the quality of the observed data (noise and zero transmission offsets), and (5) the retrieval algorithm. In contrast to previous assessments^{16,15} and where the errors were taken to be invariant as a function of altitude, we have estimated the altitude dependence of each term (illustrated in Figure 5). Table 3 summarizes the magnitude range for each term, the root sum square of the random and systematic errors, and the total uncertainty in the measurement. Two terms, the propagated temperature error and the noise error, decrease with pressure; while, the zero offset error and the assumed CO₂ profile error increase with pressure.

An assumed vertical distribution of CO₂ is used to infer the tangent pressure, and errors in this distribution introduce a systematic error into the tangent pressure measurements. In the region between 20 and 80 km where the CO₂ volume mixing ratio is essentially constant, the reported errors are 1%, and increase to 3% at lower altitudes as the CO₂ amount increases^{13,14}. Uncertainties in the assumed temperature profile vary from 2K in the troposphere to 10K at the stratopause. Temperature errors translate into intensity errors, depending on the temperature-sensitivity of the spectral feature, and hence an error in the retrieved pressure. While nonlinear, a 10K temperature error produces a 4% error in strength and a 2K temperature error leads to an error of less than 1% in strength.

Errors in the spectroscopic parameters systematically bias the tangent pressure measurements; however, measurements of many spectral features are combined and assessed for relative compatibility and may average out small differences between different laboratory measurements. Errors in the line strengths, which are generally smaller than 2.5%, translate directly into errors in the tangent pressure, while errors in the air-broadened half-widths, typically around 4%, yield errors of less than 2%. An evaluation of the potential altitude dependence based on different features with different accuracies would be quite complicated given the number of spectral features used at each altitude, hence an accuracy of 2.5% will be assumed above 25 km, and 3.0% below 25 km to allow for the impact of the half-width accuracy.

The quality of the observed data has a profound impact on the precision of any remote sensing measurement that translates the fractional opacity of the atmosphere into gas concentration or tangent pressure determinations. The atmospheric spectra obtained by the ATMOS instrument have a finite signal to noise ratio, limited primarily by the modulation efficiency of the instrument which is frequency dependent. In the best case, at frequencies between 650 and 1100 cm^{-1} the signal to noise ratio is 300:1, degrading to 50:1 between 4000 and 5000 cm^{-1} . The finite signal to noise ratio causes a random error in the measurement of a spectral feature in proportion to the fractional opacity of the microwindow. A signal to noise ratio of 100:1 and a fractional opacity of 10% will permit the measurement of the spectral feature with a precision of 10%, while at a lower altitude where the fractional opacity is larger, perhaps 30%, the precision will be 3%. Consequently, the contribution of the finite signal to noise ratio to the error budget will be strongly altitude dependent for a single line due to the coupling through the fractional opacity.

Additionally, uncertainties in the instrumental line shape function and detector response limit the quality of the spectra and hence the measurements that can be made from the spectra. The instrumental line shape is modeled in the retrieval process, and will be considered as components of the algorithm accuracy. The detector response may be nonlinear and produce an offset of the zero transmission level which alters the apparent depth of spectral features and hence the tangent pressure measurement. Abrams *et al*¹⁷ (1994) have reported a method of minimizing the effect of detector nonlinearity, and assessed the impact of zero transmission offsets on the measurement of gas concentrations. The result is a systematic error in the gas concentration which is less than 1%.

Algorithm accuracy is difficult to assess since accurate modeling of the spectral response of the instrument is critical. Small errors in line shape can alter the assessment of the gas concentration or tangent pressure. Typically, the calculated spectrum is convolved with an instrumental response function that includes the instrumental line shape and field of view. Additionally, some numerical apodization is used to enhance the signal to noise ratio in the measurement process. Comparisons with independent algorithms provide an important evaluation of the calculation of the instrumental response function; the results agree at the 1-3% level and suggest that any systematic errors present in the algorithm do not perturb the results significantly. The scaling of the precision in an occultation (signal to noise ratio of 100:1) of 2-6% to the result from a hemispheric average occultation (signal to noise of 300:1) of .5-1.5% indicates that over a large altitude range the uncertainties are dominated

by random errors due to noise in the spectra. The compatibility of the results obtained from CO₂ and N₂ suggest that the systematic error estimates in Table 3 and Figure 5 are reasonable and perhaps conservative.

The first step in the process of remote sensing of atmospheric trace gas concentrations is the determination of the viewing geometry. A spectroscopic determination, through the retrieval of the tangent pressure from the spectra in a manner that is consistent with the measurement of the trace gas burdens provides a degree of self-consistency and minimizes the potential for systematic errors. Once the tangent pressure is assigned, the measurement of constituent concentrations is straightforward. Typically, the tangent pressure errors are systematically smaller than the constituent errors because there are more spectral features with higher quality laboratory measurements. Consequently, the pressure errors, as vertical error bars, are rarely displayed or tabulated with constituent profiles. However, a 3% pressure error corresponds to a 3% error in CO₂ concentration, and should map directly into a corresponding error in the concentration of any other constituent profile. Consequently, the precision estimate in constituent measurements should be the root sum square of the pressure precision and the constituent precision,

5. Comparison with simultaneous measurements of tangent pressure and tangent temperature

An alternative method is the simultaneous determination of tangent pressure and temperature from spectroscopic measurements of CO₂ features that are both temperature-sensitive and temperature-insensitive. Rascal on a global spectral fitting approach, such a method has been applied to the ATMOS/SPACELAB-3 spectra⁵. More recently, Stiller *et al*⁶ have used the spectral fitting retrieval described in the present work to derive pressure versus temperature profiles from measurements of individual CO₂ lines and their corresponding lower state energies. The principle advantage of these methods is the determination of tangent pressure in spectral regions where there are insufficient temperature-insensitive CO₂ spectral features. Secondly, the measurement of tangent temperature with an accuracy of 2-3K between altitudes of 15 and 70 km may be desirable for certain applications where trace gas measurements can only be performed with temperature-sensitive spectral features. In spectra regions where both methods of tangent pressure measurement can be used, pressure-sounding is a simpler problem and in spectra regions where there are no temperature-sensitive spectral features available in the spectrum, the method described here may be the only practical approach

for determining reliable tangent pressures, 'This is the case, for example, in ATMOS Filter 2 covering 1100-2000 cm^{-1} .

The propagation of tangent temperature errors into constituent measurement errors is dependent on the species (through the partition function and the shape of the vertical profile) and the lower state energies of the target molecule's infrared spectral features. In addition, the wrong tangent pressure will be assigned to a spectrum if temperature-sensitive CO_2 lines are used in the pressure sounding in combination with an incorrect temperature profile. A comparison of retrievals obtained with pressure sounding based on a meteorological temperature profile and a simultaneous measurement of tangent temperature and pressure demonstrated that the choice of temperature profiles and tangent pressures does alter the form of the profiles of uncorrelated gases in a systematic fashion, but at a level that is statistically insignificant since the differences are comparable to or smaller than the precision of the measurements. In cases where both pressure sounding and simultaneous pressure temperature retrievals can be performed, the measured tangent pressures are essentially identical, and consequently the time required to achieve the result should be considered. Additionally, in the case of the ATMOS experiment, we have found that a preliminary pressure sounding is a necessary step before a simultaneous retrieval of pressure and temperature.

6. Conclusions

We have established the precision and accuracy of tangent pressure sounding for a solar occultation remote sensing experiment based on spectroscopic measurements of temperature-insensitive CO_2 spectral features and with an independent retrieval of N_2 . The method assumes a stratospheric volume mixing ratio profile of CO_2 , a correlative National Meteorological Center temperature profile, and a set of spectroscopic line parameters as the only *a priori* information. The retrieval of tangent pressure has been shown to be self-consistent with the assumed atmospheric volume mixing ratio profiles of CO_2 and N_2 . The method is robust and reasonably independent of the assumed physical model. Except for filter bandpasses containing no temperature-insensitive absorption lines, it has not been necessary to obtain spectroscopically-determined temperature profiles to proceed with the assessment of trace gas volume mixing ratio profiles.

Three conclusions are noteworthy in the context of the design of future experiments. (1) High resolution, and hence spectral selectivity permits the use of temperature-insensitive spectral features for

the assessment of the viewing geometry and gas burden in a self-consistent fashion. (2) Temperature sounding can be avoided except in cases where there are no temperature-insensitive spectral features. (3) The tradeoff between pressure sounding and simultaneous pressure-temperature sensing should include a consideration of the time required, and the goal of the measurement. For constituent retrievals in high resolution atmospheric spectra, pressure sounding offers a rapid and accurate solution, and may in practice be necessary before simultaneous retrievals of pressure and temperature.

7. Acknowledgements

This research was performed at the Jet Propulsion Laboratory, California Institute of Technology, under a contract with the National Aeronautics and Space Administration. The author wishes to acknowledge the contributions of C. B. Farmer and G. C. Toon for many enlightening discussions about spectroscopic remote sensing and detailed criticism of the manuscript. The technical support of the ATMOS Data Processing Team is acknowledged and greatly appreciated.

8. References

1. Hoke, M. L. and Shaw, J. F. I., Atmospheric Temperature Profiles and Ray Paths From Occultation Spectra, *Appl. Opt.*, 24, 1309-1312, 1985.
2. Schaffler, W. A., Shaw, J. F. I., Farmer, C. B., Effects of Systematic Errors on the Mixing Ratios of Trace Gases Obtained From Occultation Spectra, *Appl. Opt.*, 23, 2818-2826, 1984.
3. Brown, L. R., Farmer, C. B., Rinsland, C. P., and Zander, R., Remote Sensing of the Earth's Atmosphere by High Resolution Infrared Absorption Spectroscopy, *Spectroscopy of the Earth's Atmosphere and Interstellar Medium*, Academic Press, New York, 1992.
4. Park, J. H., Russell III, J. M., and Smith, M. A. H., Solar Occultation Sounding of Pressure and Temperature using Narrowband Radiometers, *Appl. Opt.*, 19, 2132-2139, 1980.
5. Rinsland, C. P., Gunson, M. R., Zander, R., and Lopez-Puertas, M., Middle and Upper Atmosphere Pressure-Temperature Profiles and the Abundances of CO₂ and CO in the Upper Atmosphere From ATMOS-Spacelab 3 Observations, *J. Geophys. Res.*, 97, 20479-20492, 1992.
6. Stiller, G. P., Gunson, M. R., Lowes, L. L., Abrams, M. C., Raper, O. F., Farmer, C. B., Zander, R., and Rinsland, C. P.; Stratospheric and Mesospheric Pressure-Temperature Profiles from the Rotational Analysis of CO₂ Lines of ATMOS/ATLAS-1 Observations, *J. Geophys. Res.*, in press, 1994.
7. Farmer, C. B., High Resolution Infrared Spectroscopy of the Sun and the Earth's Atmosphere from Space, *Mikrochim. Acts (Wien)*, 111, 189-214, 1987.
8. Gelman, M. F., personal communication, 1992.
9. Gelman, M. F., Stratospheric Monitoring with TOVS Data, *Palaeogeogr., Palaeoclimatol., Palaeoecol. (Global and Planet. Change Section)*, 90, 75-78, 1991.
10. Finger, F. G., Gelman, M. H., Wild, J. D., Chanin, M. L., Lauchecorne, A., and Miller, A. J., Evaluation of NMC Upper-Stratospheric Temperature Analyses Using Rocketsonde and Lidar Data, *Bulletin of the American Meteorological Society*, 74, 789-799, 1993.
11. Jedin, A. E., Extension of the MSIS Thermosphere Model into the Middle and Lower Atmosphere, *J. Geophys. Res.*, 96, 1159-1172, 1991.
12. Barnett, J. J. and Corney, M., Middle Atmosphere Reference Model Derived from Satellite Data, Middle Atmosphere Program Handbook, Volume 16, 47-196, 1985.

13. Bischof, W., Borchers, R., Fabian, P., and Kruger, B. C., Increased concentration and vertical distribution of carbon dioxide in the stratosphere, *Nature*, **316**, 708-710, 1985.
14. Schmidt, U. and Khedim, A., in Situ Measurements of Carbon Dioxide in the Winter Arctic Vortex and at Mid-latitudes: an indicator of the age of stratospheric air, *Geophys. Res. Lett.*, **18**, 763-766, 1991.
15. Demoulin, P., Farmer, C. B., Rinsland, C. P., and Zander, R., Determination of Absolute Strengths of N_2 Quadrupole Lines from High Resolution Ground-Based IR Solar Observations, *J. Geophys. Res.*, **96**, 13003-13008, 1991.
16. Gunson, M. R., Farmer, C. B., Norton, R. J., Zander, R., Rinsland, C. P., Shaw, J. J., and Gao, B.-c. Measurements of CH_4 , N_2O , CO , H_2O , and O_3 in the Middle Atmosphere by the Atmospheric Trace Molecule Spectroscopy Experiment on Spacelab 3, *J. Geophys. Res.*, **95**, 13,867- 13,882., 1990.
17. Abrams, M. C., Toon, G. C., and Schindler, R. A.; A Practical Example of the Correction of Fourier Transform Spectra for Detector Nonlinearity, accepted for publication in *Appl. Opt.*, 1994.

7. Figure Captions

Figure 1. Random pressure error and statistical evaluation of the pressure sounding for one solar occultation based on twelve microwindows. (a) Pressure error (solid curve) and the number of microwindows (dashed curve). (b) The CO₂ volume mixing ratio, assuming the spectroscopic tangent pressures and the weighted standard deviation of the twelve measurements compared with the assumed CO₂ volume mixing ratio profile for 1992 (solid curve), the dashed curves represent $\pm 5\%$ limits about the expected 1992 profile.

Figure 2. Pressure sounding error (precision) as a function of the number of microwindows (a nominal surrogate for the combined opacity of several microwindows). This mapping defines the upper limit of the precision as a function of the amount of information available.

Figure 3. (a) Pressure sounding errors (tangent height errors (meters) for a sunrise zonal occultation with a high signal to noise ratio (300:1). (b) The CO₂ volume mixing ratio profile and 1σ weighted standard deviation errors and the assumed CO₂ volume mixing ratio profile for 1992 (solid curve), and $\pm 5\%$ limits about the expected 1992 profile.

Figure 4. Nitrogen N₂ volume mixing ratio profiles for (a) a single occultation and (b) a mean zonal occultation compared with the assumed N₂ profile of 0.7801 (solid curves). This validation of the tangent pressures and tangent pressure errors illustrated in Figures 5 and 8 is independent of any of the assumption pertaining to the assignment of tangent pressure based on the spectroscopic measurements of CO₂. Only residual temperature and algorithm errors would effect both the CO₂ and N₂ measurements in a systematic fashion and are statistically insignificant. Notice that the horizontal scales are different, and that in (a) the dashed curves represent $\pm 5\%$ limits, and in (b) $\pm 2\%$ limits.

Figure S. The error budget for tangent pressure sounding as a function of altitude. (a) Random error terms: (i) the spectroscopic precision, (ii) propagated error from the temperature profile, (iii) the error due to the finite signal to noise ($s/n = 100:1$), (iv) the error due to the finite signal to noise ($s/n = 300:1$). (b) Systematic error terms: (i) the accuracy of the spectroscopic parameters, (ii) the accuracy of the assumed CO₂ profile, (iii) biasing due to zero transmission level offsets. (c) The root sum square of all terms as a function of altitude in the *best* and *worst* cases.

Table1: Microwindows containing CO₂ lines
utilized for pressure-sounding

Central Freq. cm ⁻¹	Full Width cm ⁻¹	E" cm ⁻¹	Altitude Range km	Isotope	Rotational Lines	Telluric Inter.
(01101)-(00001)Band						
633.87	.20	772	55-82	626	P44	
661.84	.20	106	57-85	636	R16	03
683.94	.24	-200	68-105	626	R24,R20	
684.83	.20	-400	45-70	628	R20	
686.30	.20	-400	35-65	627,628	R27,R31	
691.97	.26	363	65-105	626	R30	
693.58	.25	412	65-93	626	R32	
(10002)-(01101)Band						
644.37	.20	1106	65-100	626	Q33	
(10001)-(01101)Band						
745.25	.30	1055	50-70	626	R31	03
746.84	.30	1106	48-70	626	R33	
(00011)-(10001)Band						
934.90	.30	1751	15-50	626	P30	
936.80	.30	1705	17-50	626	P28	
938.68	.30	1662	20-W	626	P26	
940.55	.30	1622	20-50	626	P24	
942.38	.30	1586	20-52	626	P22	
944.19	.30	1552	23-53	626	P20	
945.98	.30	1521	25-53	626	P18	
947.74	.30	1494	25-54	626	P16	
949.48	.30	1470	25-54	626	P14	
951.19	.30	1449	25-55	626	P12	
952.85	.30	1431	25-53	626	P10	
954.52	.20	1416	25-52	626	P8	03
956.18	.30	1405	25-52	626	P6	03
957.78	.20	1396	25-50	626	P4	03
(10001)-(00001)Band						
1359.30	.24	331	9-32	628	P9	CH ₄
1380.00	.30	126	19-35	628	R18	H ₂ O
1384.52	.35	221	15-34	628	R24	CH ₄ ,O ₃
1385.15	.25	239	20-30	628	R25	03
1385.95	.30	258	18-32	628	R26	03

Table1: Microwindows containing CO₂ lines
utilized for pressure-sounding

Central Freq. cm ⁻¹	Full Width cm ⁻¹	E" cm ⁻¹	Altitude Range km	Isotope	Rotational Lines	Telluric Inter.
(11 102)-(00001)Band						
1909.50	.30	363	30-58	626	P30	03
1911.00	.30	317	30-58	626	P28	03
1912.52	.30	274	33-60	626	P26	O ₃ ,H ₂ O
1914.03	.30	234	35-60	626	P24	NO
1915.55	.30	197	35-60	626	P22	
1917.06	.30	164	35-63	626	P20	
1950.70	.60	197	18-32	626	R22	03
1952.31	.30	234	23-36	626	R24	
1953.92	.30	274	23-36	626	R26	
(1 1101)-(00001)Band						
2055.16	.30	317	50-73	626	P28	
2056.70	.30	274	50-75	626	P26	03
2058.24	.30	223	50-75	626	P24	03
2061.32	.30	164	50-76	626	P20	03
2076.85	.90	0-135	50-78	626	Q2-Q18	
(00011)-(00001)Band						
2314.58	.20	186	60-92	628	P22	H ₂ O
2315.48	.20	170	70-95	628	P21	
2316.62	.20	307	60-80	627	P28	
2328.67	.20	234	76-125	626	P24	
2332.37	.30	164	78-125	626	P20	
2364.10	.30	164	80-125	626	R20	
2366.65	.30	234	78-125	626	R24	
2369.08	.30	317	78-125	626	R28	
2372.56	.30	464	74-120	626	R34	
(21 103)-(00001)Band						
3204.75	.40	317	15-30	626	R28	C ₂ H ₂
3206.41	.40	363	13-30	626	R30	
3211.38	.40	520	15-25	626	R36	

Table 1: Microwindows containing CO₂ lines
utilized for pressure-sounding

Central Frequ. cm ⁻¹	Full Width cm ⁻¹	E" cm ⁻¹	Altitude Range km	Isotope	Rotational Lines	Telluric inter,
(21 102)-(00001) Band						
3312.63	.40	464	20-38	626	P34	
3315.79	.35	363	22-42	626	P30	
3318.95	.30	274	2240	626	P26	
3322.11	.30	197	21-42	626	P22	
3323.68	.40	164	18-38	626	P20	
3325.25	.40	133	20-38	626	P18	
3351.07	.25	814	8-30	626	R14	
3352.52	.25	1064	8-30	626	R16	
3354.10	.40	1334	8-30	626	R18	
3357.30	.40	1975	2-45	626	R22	
3358.70	.40	2345	2-38	626	R24	
3361.85	.30	3165	2-38	626	R28	
3363.32	.35	3625	2-30	626	R30	
(1001 2)-(00001) Band						
3511.17	.35	163	72-50	636	P20	
3516.51	.40	81	72-50	636	P14	
3518.02	.25	60	72-50	636	P12	
3535.97	.24	43	72-50	636	R10	

Table2: Microwindows containing N2 lines
utilized for pressure-sounding

Central Frequ. cm ⁻¹	Full Width cm ⁻¹	E " cm ⁻¹	Altitude Range km	Isotope	Rotational Lines	Telluric Inter.
2395.97	.80	111	16-38	14	S7	O ₃ ,N ₂ O,CH ₄
2403.57	.80	143	16-40	14	S8	O ₃ ,N ₂ O
2411.13	.70	179	16-35	14	S9	O ₃ ,N ₂ O
2418.65	.84	219	16-40	14	S10	O ₃ ,N ₂ O

Table 3: Error Budget for Tangent Pressure Sounding

Error Source	Error Type	Range (%)
Temperature Profile	R	1-2
CO2 Profile	s	1-3
Reference Pressure	s	2
Spectroscopic Parameters	s	2.5-3.0
S/N(100,300)	R	1.0-10.0, 0.3-3.0
Zero Offsets	R	<1
Algorithm	s	1-3
Total Systematic Error		4, 8 - 6 . 7
Total Random Error		0.4-10.1, 1.0-3.6
Total Uncertainty		5.0-11, 4.9-7.6

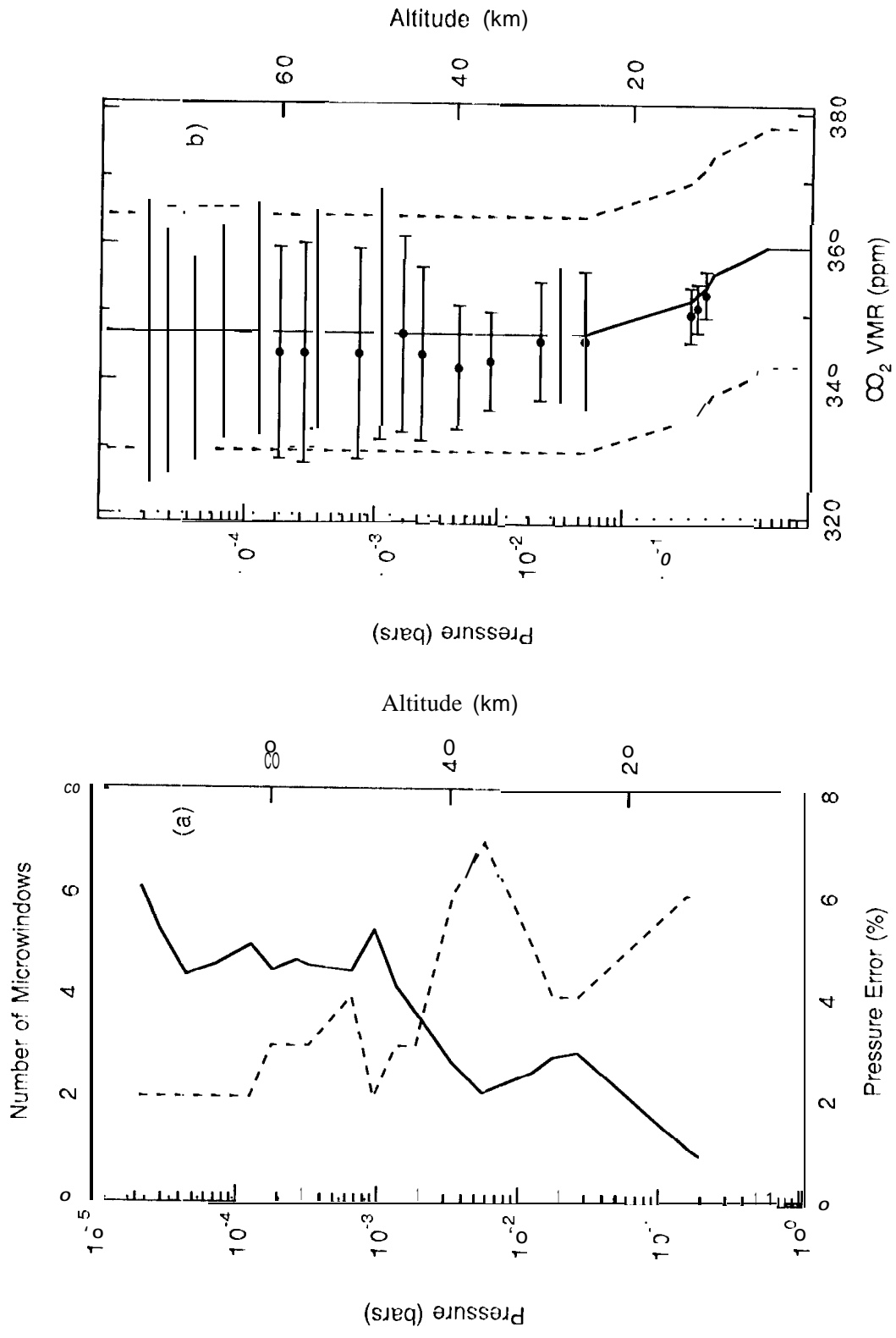


Figure 1

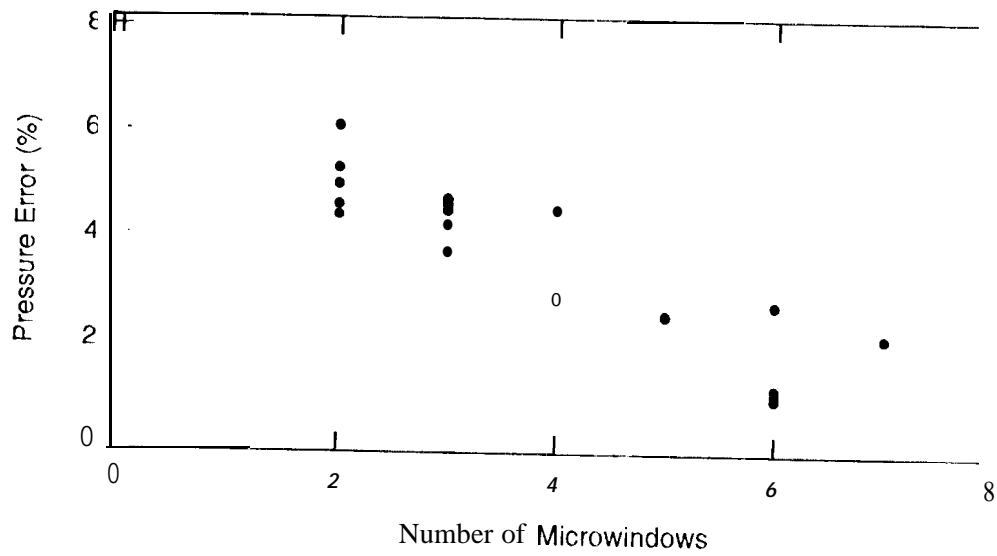


Figure 2.

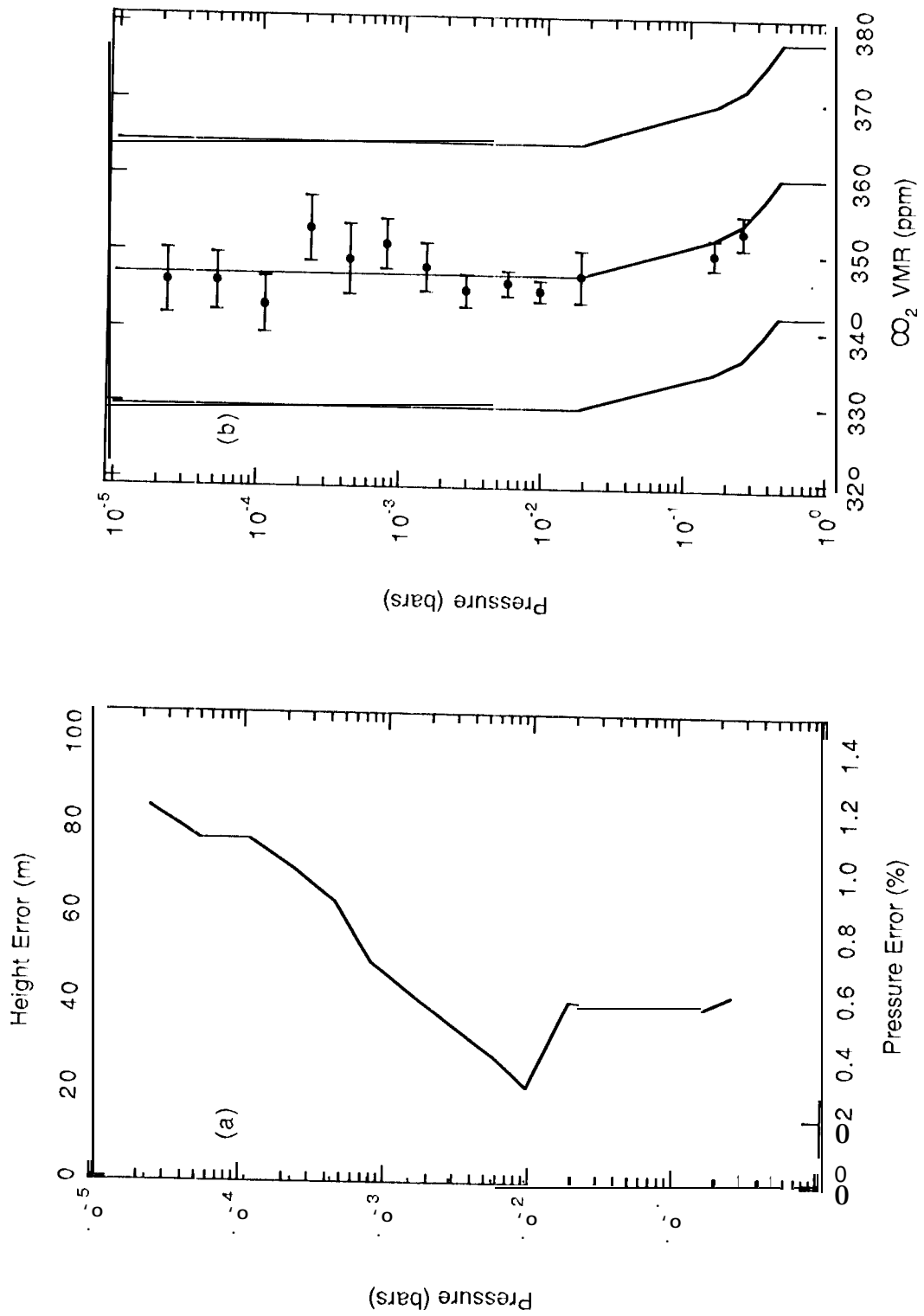


Figure 3.

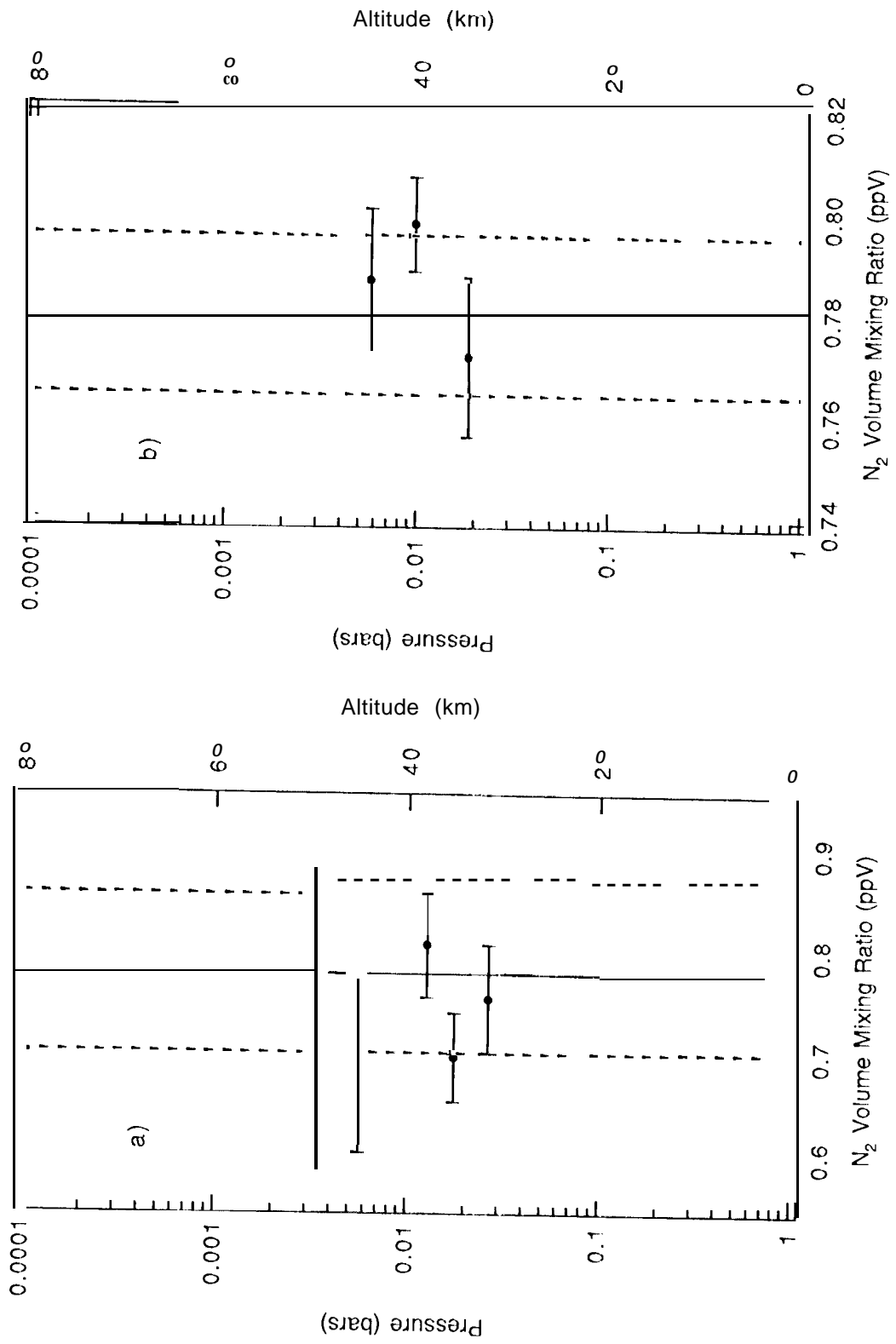


Figure 4.

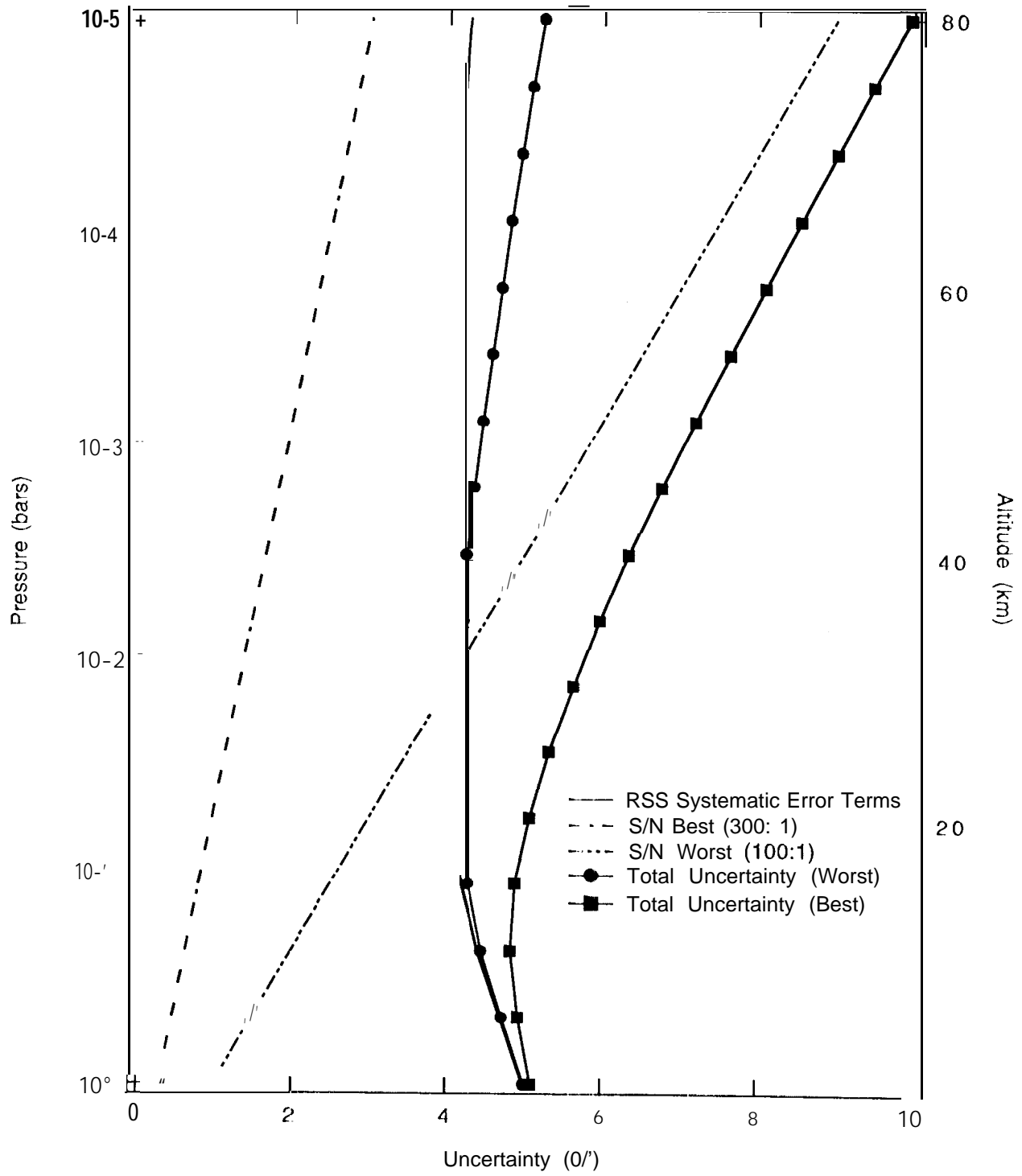


Figure 5.